ARCHIVES OF ELECTRICAL ENGINEERING VOL. 67(2), pp. 403–417 (2018)

DOI 10.24425/119649

An observer for magnetic levitation system control based on a coefficient diagram method and backstepping

Fouad Haouari[1], **Nourdine Bali**[2], **Mohamed Tadjine**[1], **Mohamed Seghir Boucherit**[1]

[1] *Department of Electrical Engineering, Process Control Laboratory, ENP*
10. avenue Hassan Badi P.O Box 182 Algiers, Algeria, 16200

[2] *Electrical Engineering and Computing Faculty*
USTHB P.O Box 32 El Alia, Bab Ezzouar Algiers, 16111 Algeria
e-mail: haouari_fouad@yahoo.fr

(Received: 18.09.2016, revised: 19.03.2018)

Abstract: In this paper, we propose a robust nonlinear control design concept based on a coefficient diagram method and backstepping control, combined with a nonlinear observer for the magnetic levitation system to achieve precise position control in the existence of external disturbance, parameters mismatch with considerable variations and sensor noise in the case, where the full system states are supposed to be unavailable. The observer converges exponentially and leads to good estimate as well as a good track of the steel ball position with the reference trajectory. A simulation results are provided to show the excellent performance of the designed controller.

Key words: backstepping, coefficients diagram method controller, magnetic levitation system, nonlinear observer

1. Introduction

Magnetic levitation systems are needed in various industrial applications, e.g., frictionless bearings, high-speed maglev passenger trains, vibration isolation of sensitive machinery [1–3], etc. These systems are characterized by a narrow travel range, open loop instability, highly nonlinear dynamics [4] and some of their dynamic parameters are uncertain, subsequently, the problem of designing of a robust controller is essential. Several control techniques have been planned for the control of a magnetic levitation system in the past. The classical proportional, integral and derivative (PID) controller can be used in the position control, but this technique may not achieve best performance requirements due to the presence of nonlinear dynamics inherent in this range of systems. In fact, the classical PID scheme necessitates the linearization of the system dynamics around an operating point and requires the exact knowledge of system parameters. The sliding mode control may lead to considerable control efforts and chattering control response, whereas the adaptive control exhibits unsatisfactory transient performance. In other study a feedback linearization controller is presented; but the controller is sensitive for parameters mismatch. As a result, attention should be paid to defeat these problems. However, in order to realize advanced concepts of the control, the acquaintance of state variables is not generally available; this can be attained by means of state observers.

In order to resolve the last well-known problems, a nonlinear robust tracking controller is created by combining the coefficient diagram method (CDM) [5–9] and backstepping procedure [10–18] (CDM-backstepping) to keep almost all the robustness properties in the presence of considerable variations in parametric mismatches, external disturbances and sensor noise with exponential convergence. CDM-backstepping by means of a nonlinear observer is founded to control the position of the steel ball for the interested system. This method of control is a rigorous and procedure design methodology for nonlinear feedback control. It is a recursive technique [10, 11] based on the Lyapunov stability method [12–15], which consists of iterative steps. It includes the accomplishment of global stability by describing an error variable and a corresponding stabilizing function of each subsystem to realize the control law. The approach also permits the insertion of additional nonlinearities into the control laws for elimination of disagreeable ones. Most of the control algorithms need to be implemented through digital devices. For this reason, a discrete-time controller based on Euler approximation is briefly described. The precision of the position control and the convergence of the estimated errors can be confirmed by the proposed controller.

The paper is organized as follows: section 2 presents the state space model of the interested plant. Section 3 briefly describes the CDM controller in the case of a linear system. In section 4 a nonlinear observer is proposed for the considered system. Next, stability is proven using the Lyapunov stability analysis. In section 5 the nonlinear controller coefficient diagram method based on backstepping with the nonlinear observer is described by using the Lyapunov stability. Section 6 describes the discrete CDM-backstepping by using the Euler method. In section 7 the results of the simulations are discussed, then conclusions are drawn in section 8.

2. Magnetic levitation state space model

The state space model of the magnetic levitation system shown in Fig. 1 is described as [2]:

$$\begin{cases} \dot{x}_1 = x_2 \\ \dot{x}_2 = g - \dfrac{Qx_3^2}{2M(X_\infty + x_1)^2} \\ \dot{x}_3 = \dfrac{x_3(Qx_2 - R(X_\infty + x_1)^2)}{Q(X_\infty + x_1) + L_\infty(X_\infty + x_1)^2} + \dfrac{(X_\infty + x_1)}{Q + L_\infty(X_\infty + x_1)} u \end{cases} . \tag{1}$$

where: x_1 is the vertical position of the steel ball, x_2 is the speed of the steel ball, x_3 is the coil current, g is the gravitational acceleration, M is the mass of the steel ball, R is the electrical resistance, u is the voltage control input, L_∞, Q and X_∞ are positive constants established by the characteristics of the coil, magnetic core, and steel ball, respectively.

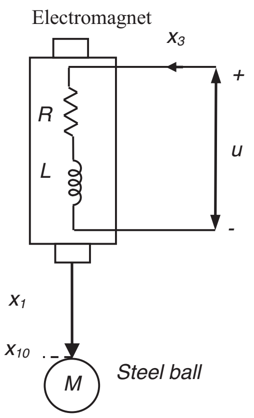

Fig. 1. System diagram and coordinate system

3. CDM control design

The coefficient diagram method is an algebraic method applied to a polynomial loop in the parameters space [5]. This controller gives the system response of the controlled system, fulfilling both transient and steady state response requirements. Stability and speed are designed from the standard stability index and the equivalent time constant respectively. When the settling time of the controlled system has been chosen, the equivalent time constant is achieved.

Consider the mathematical model of a linear, time invariant system, described in a transfer function as follows:

$$R(s) = \frac{N(s)}{D(s)} = \frac{a_m s^m + a_{m-1} s^{m-1} + \ldots + a_0}{b_n s^n + b_{n-1} s^{n-1} + \ldots b_0}\,. \tag{2}$$

$N(s)$ and $D(s)$ are the numerator and the denominator of the system transfer function.

From Fig. 2, the output y of the controlled closed loop system can be expressed as:

$$y = \frac{N(s)F(s)}{P(s)} r + \frac{A(s)N(s)}{P(s)} d, \tag{3}$$

where: y is taken as the output of the controlled system, r is denoted as the reference input to the system, u is the control signal, d is the external disturbance signal, $F(s)$ is called the reference numerator of the controller. While $P(s)$ is the characteristic polynomial [5] of the closed loop system and is formulated as follows:

$$P(s) = D(s)A(s) + N(s)B(s) = \sum_{i=0}^{n} \mu_i s^i, \tag{4}$$

where μ_i are the coefficients of $P(s)$.

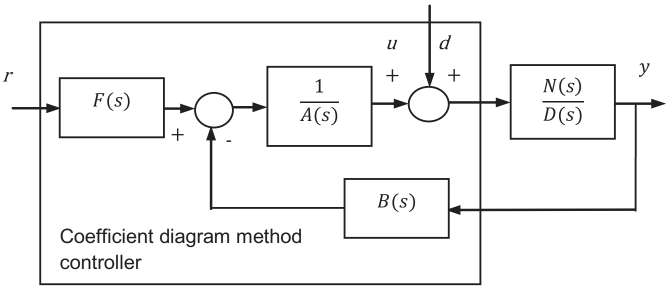

Fig. 2. A block diagram of a CDM control system

The polynomials $A(s)$ and $B(s)$ are the controller polynomials [6] and are expressed as:

$$A(s) = \sum_{i=0}^{n} l_i s^i \qquad \text{and} \qquad B(s) = \sum_{i=0}^{n} q_i s^i,$$

where: l_i and q_i are the controller parameters.

Controlling with the CDM necessitates some design parameters which are represented by the equivalent time constant τ to designate the speed of time response in the closed loop and the stability indices γ_i to provide the stability and the shape of the closed loop response.

They are related to the coefficients of the characteristic polynomial [7] specified in (4) as:

$$\tau = \mu_1/\mu_0 \quad \text{and} \quad \gamma_i = \mu_i^2/\mu_{i-1}\mu_{i+1} \qquad \text{for } i \in [1\ n-1].$$

The relation between the settling time t_s and the equivalent time constant is given as follows:

$$\begin{cases} \tau = \dfrac{t_s}{(2.5\sim3)} \\ \gamma_1 = 2.5, \quad \gamma_i = 2, \quad i \in [2\ n-1], \quad \gamma_0 = \gamma_n = \infty \end{cases}. \tag{5}$$

The stability limit values can be changed by the designer as per the requirement in robustness by using $\gamma_i > 1.5\gamma_i^*$ with $i \in [1\ n-1]$. The characteristic polynomial [6, 7], can be defined as:

$$P(s) = \mu_0 \left[\left\{ \sum_{i=2}^{n} \prod_{j=1}^{i-1} \frac{1}{\gamma_{i-j}^{j}} (\tau_0 s)^i \right\} + \tau s + 1 \right]. \tag{6}$$

The reference numerator polynomial $F(s)$ is a pre-filter [6], it can be defined as follows:

$$F(s) = \frac{P(s)|_{s=0}}{N(s)}. \tag{7}$$

4. Observer design and stability analysis

In the following, we design and prove the exponential stability of the nonlinear observer, based on the backstepping method for the Lipschitz nonlinear system [19].

Let us consider the Lipschitz nonlinear system given as follows:

$$\begin{cases} \dot{x} = Ax + Bu + \phi(x,u) \\ y = x_1 \end{cases}, \tag{8}$$

where the pair (A, B) is controllable and the pair (C, A) is observable.

The observer given by (9) can be proposed for the Lipschitz nonlinear system specified by (8) as:

$$\dot{\hat{x}} = A\hat{x} + Bu + \phi(\hat{x}, u) + H(y - \hat{x}_1), \tag{9}$$

where H is the observer gain vector and $\phi(x,u)$ is Lipschitz with respect to the state x, uniformly in the control u, that is, there exists a constant η such that

$$\begin{cases} \|\phi(x_1,u) - \phi(x_2,u)\| \le \eta\|x_1 - x_2\|, & \forall x_1, x_2 \in R^3, \;\; u \in R \\ \|\phi(x,u)\| \le \eta\|x\|, & \forall u \in R \end{cases}. \tag{10}$$

Let the estimation error $e_o = x - \hat{x}$, its dynamics is given as:

$$\dot{e}_o = \dot{x} - \dot{\hat{x}} = (A - H)e_o + \phi(x,u) - \phi(\hat{x},u) = A_o e_o + \phi(x,u) - \phi(\hat{x},u). \tag{11}$$

Consider the following Lyapunov function candidate $V_o = e_o^T P e_o$, where $P = P^T$, its time derivative is specified as:

$$\dot{V}_o = e_o^T \left(A_o^T P + PA_o\right) e_o + 2e_o^T P\left(\phi(x,u) - \phi(\hat{x},u)\right). \tag{12}$$

Using (10), gives

$$\dot{V}_o \le e_o^T \left(A_o^T P + PA_o\right) e_o + 2\eta\|Pe_o\|\,\|e_o\|. \tag{13}$$

Completing squares on the term $2\eta\|Pe_o\|\,\|e_o\|$, for any $\alpha > 0$, we obtain:

$$\dot{V}_o = e_o^T (A_o^T P + PA_o + PP + \eta^2 I)e_o. \tag{14}$$

Then $A_o^T P + PA_o + PP + \eta^2 I = -\alpha I$, afterward

$$\dot{V}_o \le -\alpha e_o^2. \tag{15}$$

The considered system (1) is rewritten in the next form to verify the conditions of controllability and observability given previously.

$$\begin{cases} \dot{x}_1 = x_2 \\ \dot{x}_2 = x_3 + g - \dfrac{Qx_3^2 + 2Mx_3(X_\infty + x_1)^2}{2M(X_\infty + x_1)^2} \\ \dot{x}_3 = \dfrac{x_3(Qx_2 - R(X_\infty + x_1)^2)}{Q(X_\infty + x_1) + L_\infty(X_\infty + x_1)^2} + \dfrac{1}{L_\infty}u - \dfrac{1}{L_\infty}\dfrac{Q}{Q + L_\infty(X_\infty + x_1)}u \end{cases}. \tag{16}$$

Taking

$$f_1(x) = g - \frac{Qx_3^2 + 2Mx_3(X_\infty + x_1)^2}{2M(X_\infty + x_1)^2},$$

$$g(x) = -\frac{1}{L_\infty}\frac{Q}{Q + L_\infty(X_\infty + x_1)}$$

and

$$f_2(x) = \frac{x_3(Qx_2 - R(X_\infty + x_1)^2)}{Q(X_\infty + x_1) + L_\infty(X_\infty + x_1)^2}.$$

State space model (16) can be simplified as:

$$\begin{cases} \dot{x}_1 = x_2 \\ \dot{x}_2 = x_3 + f_1(x) \\ \dot{x}_3 = f_2(x) + \dfrac{1}{L_\infty}u + g(x)u \end{cases} . \tag{17}$$

Then

$$A = \begin{bmatrix} 0 & 1 & 0 \\ 0 & 0 & 1 \\ 0 & 0 & 0 \end{bmatrix}, \quad B = \begin{bmatrix} 0 \\ 0 \\ 1/L_\infty \end{bmatrix}, \quad C^T = \begin{bmatrix} 1 \\ 0 \\ 0 \end{bmatrix}, \quad \phi(x,u) = \begin{bmatrix} 0 \\ f_1(x) \\ f_2(x) + g(x)u \end{bmatrix}. \tag{18}$$

Tacking the nominal physical parameters M_0, R_0, Q_0, M_{∞_0}, L_{∞_0} and X_{∞_0}, we have the following nominal nonlinear functions:

$$f_{10}(x) = g - \frac{Q_0 x_3^2 + 2M_0 x_3 (X_{\infty_0} + x_1)^2}{2M_0(X_{\infty_0} + x_1)^2},$$

$$f_{20}(x) = \frac{x_3(Q_0 x_2 - R_0(X_{\infty_0} + x_1)^2)}{Q_0(X_{\infty_0} + x_1) + L_{\infty_0}(X_{\infty_0} + x_1)^2},$$

$$g_0(x) = -\frac{1}{L_{\infty_0}}\frac{Q_0}{Q_0 + L_{\infty_0}(X_{\infty_0} + x_1)}.$$

The model mismatches between the real system and the supposed nominal are given as:

$$\Delta_{f1}(x) = f_1(x) - f_{10}(x),$$

$$\Delta_{f2}(x) = f_2(x) - f_{20}(x)$$

and

$$\Delta_g(x) = g(x) - g_0(x).$$

5. CDM-backstepping control with nonlinear observer

The development of the exponential stability of the nonlinear observer in the previous section is independent of the control input. In this section, the nonlinear observer is composed with the CDM-backstepping control to explore the feedback control as illustrated in Fig. 3.

The control objective is to design a control law to oblige the steel ball to track exponentially a reference position input.

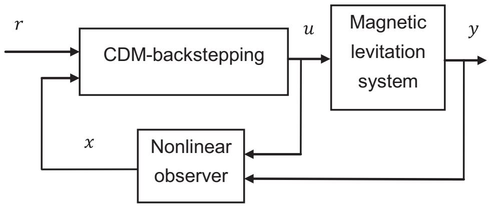

Fig. 3. Scheme of CDM-backstepping controller with nonlinear observer

The nonlinear observer (19) is used to estimate the state of the considered system

$$\begin{cases} \dot{\hat{x}}_1 = \hat{x}_2 + h_1(y - \hat{x}_1) \\ \dot{\hat{x}}_2 = \hat{x}_3 + f_1(\hat{x}) + h_2(y - \hat{x}_1) \\ \dot{\hat{x}}_3 = f_2(\hat{x}) + g(\hat{x})u + h_3(y - \hat{x}_1) \end{cases} . \tag{19}$$

where the observer gain vector is $H = (h_1\ h_2\ h_3)^T$.

The procedure for demonstrating the stability is pretty much the same with respect to conventional backstepping, only some important changes occur at the final step, when the nonlinear CDM can be developed. We maintain the same terminology definitions like virtual control, but add some new ones like parameters of adjustment. The procedure can be developed in 3 steps.

In the first step, let us take into consideration only the first equation of (19), then consider the position error z_1 given as $z_1 = \hat{x}_1 - x_d$, where x_d is the reference signal, its time derivative is $\dot{z}_1 = \dot{\hat{x}}_1 - \dot{x}_d = \hat{x}_2 + h_1 e_{o1} - \dot{x}_d$.

The first candidate Lyapunov function is selected as $V_1 = 0.5z_1^2 + V_o$, its derivative is given as:

$$\dot{V}_1 = z_1\dot{z}_1 + \dot{V}_o\,. \tag{20}$$

Using Equation (15), one has

$$\dot{V}_1 \leq z_1\dot{z}_1 - \alpha V_o = z_1\left(\hat{x}_2 + h_1 e_{o1} - \dot{x}_d\right) - \alpha V_o\,. \tag{21}$$

Choosing the first stabilizing function $\phi_1 = -c_1 z_1 + \dot{x}_d$ and tacking $z_2 = \hat{x}_2 - \phi_1$, one has

$$\dot{V}_1 \leq z_1(z_2 + h_1 e_{o1} - c_1 z_1) - \alpha V_o = -c_1 z_1^2 + z_1 z_2 + h_1 e_{o1} z_1 - \alpha V_o\,, \tag{22}$$

where the second observer error is $e_{o2} = x_2 - \hat{x}_2$.

Using the generic inequality $e_{o1} z_1 \leq \kappa_1 z_1^2 + \dfrac{1}{4\kappa_1} e_{o1}^2$, with $\kappa_1 > 0$, tacking $h_1 > 0$, one has

$$\dot{V}_1 \leq -(c_1 - h_1\kappa_1)z_1^2 + z_1 z_2 + \frac{h_1}{4\kappa_1}e_{o1}^2 - \alpha V_o \leq -(c_1 - h_1\kappa_1)z_1^2 + z_1 z_2 - \left(\alpha - \frac{h_1}{4\kappa_1}\right)e_{o1}^2\,. \tag{23}$$

If we tack $\alpha > h_1/4\kappa_1$ and $c_1 > h_1\kappa_1$ with an appropriate choice of h_1 and κ_1, we obtain:

$$\dot{V}_1 \leq -\bar{c}_1 z_1^2 + z_1 z_2\,, \qquad \bar{c}_1 = c_1 - h_1\kappa_1 > 0. \tag{24}$$

For the second step, let us consider the subsystem containing the first two equations of (19) and select the second Lyapunov function as $V_2 = V_1 + 0.5z_2^2 + V_o$, its derivative is written as:

$$\dot{V}_2 = \dot{V}_1 + z_2\dot{z}_2 + \dot{V}_o \leq -\bar{c}_1 z_1^2 + z_1 z_2 + z_2\dot{z}_2 - \alpha V_o\,, \tag{25}$$

where

$$\begin{cases} \dot{z}_2 = \dot{\hat{x}}_2 - \dot{\phi}_1 = f_1(\hat{x}) + h_2 e_{o1} - \dot{\phi}_1 \\ \dot{\phi}_1 = -c_1\dot{z}_1 + \ddot{x}_d = -c_1(\dot{\hat{x}}_1 - \dot{x}_d) + \ddot{x}_d = -c_1\hat{x}_2 - c_1 h_1 e_{o1} + c_1\dot{x}_d + \ddot{x}_d \end{cases}. \tag{26}$$

Substituting (26) into (25) gives

$$\dot{V}_2 \leq -\bar{c}_1 z_1^2 + z_1 z_2 + z_2\left(f_1(\hat{x}) + c_1\hat{x}_2 + (c_1 h_1 + h_2)e_{o1} - c_1\dot{x}_d - \ddot{x}_d\right) - \alpha V_o\,. \tag{27}$$

Now, the desired control input ϕ_2 of $\hat{x}_3$ is chosen as:

$$\phi_2 = \hat{x}_3 - f_1(\hat{x}) - z_1 - c_2 z_2 - c_1\hat{x}_2 + (c_1 h_1 + h_2)e_{o1} + c_1\dot{x}_d + \ddot{x}_d\,. \tag{28}$$

Define the tracking error $z_3 = \hat{x}_3 - \phi_2$, substituting the term of ϕ_2 in (27), then

$$\dot{V}_2 \leq -\bar{c}_1 z_1^2 - c_2 z_2^2 + z_2 z_3 - \alpha V_o\,. \tag{29}$$

Subsequently, $\dot{V}_2 \leq -\bar{c}_1 z_1^2 - c_2 z_2^2 + z_2 z_3$.

In the third step of design procedure, let us consider the complete system (19) and tacking the third Lyapunov function $V_3 = V_2 + 0.5z_3^2 + V_o$, then

$$\dot{V}_3 \leq -\bar{c}_1 z_1^2 - c_2 z_2^2 + z_2 z_3 + z_3\dot{z}_3 - \alpha V_o\,. \tag{30}$$

Define the stabilizing control law ϕ_2 and the tracking error as:

$$z_3 = \hat{x}_3 - \phi_2\,. \tag{31}$$

Its derivative is expressed as:

$$\dot{z}_3 = \dot{\hat{x}}_3 - \dot{\phi}_2\,. \tag{32}$$

Then, one has

$$\dot{V}_3 \leq -\bar{c}_1 z_1^2 - c_2 z_2^2 + z_2 z_3 + z_3\dot{z}_3 - \alpha V_o\,. \tag{33}$$

Taking into consideration the virtual control $\hat{\zeta} = \hat{x}_3$, this provides $\dot{\hat{\zeta}} = f_o(\hat{x}) + g(\hat{x})u$, where $f_o(\hat{x}) = f_2(\hat{x}) + h_3 e_{o1}$, after that, the control law based on the nonlinear CDM can be formulated as:

$$a_{o0}(\hat{x})u + a_{o1}(\hat{x})\frac{\mathrm{d}u}{\mathrm{d}t} = z_o(t), \tag{34}$$

where

$$z_o(t) = c_{o0}(\hat{x})\phi_2 - b_{o0}(\hat{x})\hat{\zeta} - b_{o1}(\hat{x})\dot{\hat{\zeta}}\,. \tag{35}$$

The terms $a_{o0}(\hat{x})$, $a_{o1}(\hat{x})$, $c_{o0}(\hat{x})$, $b_{o0}(\hat{x})$ and $b_{o1}(\hat{x})$ represents the nonlinear gains of the nonlinear CDM controller in the company of the observer.

Consider the observer specified by (19) with the CDM control given by (34) and (35) and presume that the gains δ_{o0} and c_{o0} are such that

$$\left| c_{o0}\delta_{o0}\,\mathrm{sign}(z_s)\int_0^t z_3(\sigma)\,\mathrm{d}\sigma \right| \geq |z_2| + |h_o(\hat{x})|\,, \tag{36}$$

where $\mathrm{sign}(z_s) = +1$ if $z_s > 0$, $\mathrm{sign}(z_s) = 0$ if $z_s = 0$ and $\mathrm{sign}(z_s) = -1$ if $z_s < 0$.

Then, we can create the control signal to ensures the asymptotic convergence of $z_3(t)$.

Tacking the k_o positive constant to select the nonlinear gains as follows:

$$\begin{cases} a_{o0}(\hat{x}) = -k_o \dfrac{\mathrm{d}g(\hat{x})}{\mathrm{d}t} \\ a_{o1}(\hat{x}) = -k_o g(\hat{x}) \end{cases}. \tag{37}$$

After that, combining (31) with (35), results in

$$z_3 = (c_{o0}b_{o0}^{-1} - 1)\phi_2 - b_{o0}^{-1} z_o\,. \tag{38}$$

Afterward, tacking $c_{o0}(\hat{x}) = b_{o0}(\hat{x}) = c_{o0}$ as constants and $b_{o1}(\hat{x}) = 0$, one has

$$z_o = -c_{o0}z_3\,. \tag{39}$$

Then compute the second time derivative of z_o as follows:

$$\ddot{z}_o = c_{o0}\ddot{\phi}_2 - c_{o0}\ddot{\xi}(t). \tag{40}$$

Combining (34) with (35) and using (37), gives

$$\ddot{\xi}(t) = \dot{f}_o(\hat{x}) - k_{o1}z_o\,, \tag{41}$$

where $k_{o1} = k_o^{-1}$ after that, substituting (41) into (40), gives

$$\ddot{z}_o = c_{o0}\ddot{\phi}_2 - c_{o0}(\dot{f}_o(\hat{x}) - k_{o1}z_o). \tag{42}$$

Subsequently

$$\dot{z}_o = c_{o0}\dot{\phi}_2 - c_{o0}\left(f_o(\hat{x}) - k_{o1}\int_0^t z_o(\sigma)\,\mathrm{d}\sigma \right). \tag{43}$$

Introducing (39) into (43) provides

$$\dot{z}_3 = h_o(\hat{x}) - k_{o2}\int_0^t z_3(\sigma)\,\mathrm{d}\sigma\,, \tag{44}$$

where: $k_{o2} = c_{o0}k_{o1}$ and $h_o(\hat{x}) = f_o(\hat{x}) - \dot{\phi}_2(t)$.

Supposing that $k_{o2} = \delta_{o0}\,\mathrm{sign}\,(z_s)$, the related constants are $k_{o1} = \frac{\delta_{o0}}{c_{o0}}\,\mathrm{sign}\,(z_s)$ and $k_o = \frac{c_{o0}}{\delta_{o0}}\,\mathrm{sign}\,(z_s)$, then, we take that $z_s = z_3 \int_0^t z_3(\sigma)\,\mathrm{d}\sigma$ and if we insert (44) into (33), it gives us:

$$\dot{V}_3 \leq -\bar{c}_1 z_1^2 - c_2 z_2^2 + z_2 z_3 + z_3 \left(h_o(x) - k_{o2} \int_0^t z_3(\sigma)\,\mathrm{d}\sigma \right) - \alpha V_o \leq -\bar{c}_1 z_1^2 - c_2 z_2^2 + v_o(t), \quad (45)$$

with

$$v_o(t) = z_3 \left(z_2 + h_o(x) - k_{o2} \int_0^t z_3(\sigma)\,\mathrm{d}\sigma \right) = z_3 (z_2 + h_o(x) - c_{o0}\delta_{o0} z_s\,\mathrm{sign}\,(z_s)).$$

While the function $z_s\,\mathrm{sign}\,(z_s)$ at all times is positive, $v_o(t)$ is negative, if the gains δ_{o0} and c_{o0} are selected with respect to inequality (36), they are adjusted till acceptable results are achieved, at last, we obtain $\dot{V}_3 \leq -\bar{c}_1 z_1^2 - c_2 z_2^2$, or $\dot{V}_3$ negative definite. This indicates the exponential convergence to zero of the tracking error. As a result, the position control with the nonlinear observer of the considered system is realized.

6. Discrete CDM-backstepping controller

The Euler approximation for the interested system given by (17) and the observer given by (19) are represented by (46) and (47), respectively.

$$\begin{cases} x_1(j+1) = x_1(j) + T_s x_2(j) \\ x_2(j+1) = x_2(j) + T_s x_3(j) + T_s f_1(x(j)) \\ x_3(j+1) = x_3(j) + T_s f_2(x(j)) + \dfrac{T_s}{L_\infty} u(j) + T_s g(x(j)) u(j) \end{cases}, \quad (46)$$

$$\begin{cases} \hat{x}_1(j+1) = \hat{x}_1(j) + T_s \hat{x}_2(j) + T_s h_1(y(j) - \hat{x}_1(j)) \\ \hat{x}_2(j+1) = \hat{x}_2(j) + T_s \hat{x}_3(j) + T_s f_1(\hat{x}(j)) + T_s h_2(y(j) - \hat{x}_1(j)) \\ \hat{x}_3(j+1) = \hat{x}_3(j) + T_s f_2(\hat{x}(j)) + T_s g(\hat{x}(j)) u(j) + T_s h_3(y(j) - \hat{x}_1(j)) \end{cases}, \quad (47)$$

where T_s is the sufficiently short sampling time.

The discrete control law for a magnetic levitation system is given as:

$$\begin{cases} u(j+1) = \left(1 - T_s \dfrac{a_{o0}(\hat{x}(j))}{a_{o1}\hat{x}(j)}\right) u(j) + \dfrac{T_s}{a_{o0}(\hat{x}(j))} \hat{z}_o(j) \\ \hat{\zeta}(j+1) = \left(1 - T_s \dfrac{b_{o0}(\hat{x}(j))}{b_{o1}\hat{x}(j)}\right) \hat{\zeta}(j) + \dfrac{T_s c_{o0}(\hat{x}(j))}{b_{o1}(\hat{x}(j))} \phi_2(\hat{x}(j)) - \dfrac{T_s}{b_{o1}(\hat{x}(j))} \hat{z}_o(j) \end{cases}. \quad (48)$$

7. Simulation result

To test the suggested control procedure, we plot two tests, which are illustrated in Fig. 4 and Fig. 5, in order to display the robustness and performance in terms of time response and the convergence of the estimation and tracking errors for the observer as well as the controller. The reference to a position can be created by applying a sequence of three different sine waves in frequency bands. In the first test, this reference signal has an amplitude of 5 mm and a nominal position of 5 mm.

When it has an amplitude of 4.5 mm and a nominal position of 4.5 mm in the second test, the controller is discretised with a sampling time T of 0.5 ms. The simulation is provided in a small range of motion to use the electromagnet with low cost and simple construction.

Initial conditions on states are the property of the system and are set to be zero $x(0) = (0\,0\,0)^T$ in the first test and $x(0) = (1\ 0\ 0)^T$ in the second test, when the initial estimated states are chosen $\hat{x}(0) = (2\ 0\ 0)^T$ in the vicinity of the actual state $x(0)$ to ensure good performance results. The CDM gains are adjusted with respect to inequality (36) and modest $\delta_{o0} = 3.1$ and $c_{o0} = 1.4$ are selected to avoid noisy or considerable control efforts and the observer gain vector $H = (h_1\ h_2\ h_3)^T$ is chosen such that the matrix $A - BH$ is stable. In addition, high observer gains help decrease the influences of disturbance and model mismatch and is taken as $H = (1\ 2.2\ 6.1\ 0.9)^T$. However, the parameters of the controller c_1 and c_2 are relatively selected $c_1 = 35$, $c_2 = 35$, to guarantee small error signals, without causing considerable amplitude of the control input.

The parameters of the magnetic levitation system are set as follows [2]:
$M = 0.54$ kg, $g = 9.81$ m/s^2, $X_\infty = 0.008114$ m, $Q = 0.001624$ H·m, $L_\infty = 0.7987$ H, $R = 11.88\ \Omega$.

Test one: ideal case. In the first test of simulations, only nonzero initial errors have considered, and all other conditions are considered as an ideal one, that is, the observer model is an accurate equivalent to the system, no external disturbances, and no parameters mismatch.

Fig 4a, 4c and 4e shows the estimated states and the actual states. The observer errors are displayed in Fig 4b, 4d and 4e. We can observe that the estimated position tracks the actual position exponentially, this property is ensured for speed and coil current, also the observer error of all states converges to zero exponentially. Fig. 4g illustrates the behaviour of the input control voltage. Indeed, it appears clearly that the obtained input control signal is acceptable.

Test two: robustness to external disturbance, parameters mismatch with considerable nonlinear variation and sensor noise.

We disturb the output of system with sinusoidal external disturbance $d(t) = 1.5 + \sin(2\pi t)$, designated in Fig. 5h, at initial time and the following nominal system parameters with considerable nonlinear variation were employed for simulation studies: to confirm the robustness of the controllers to parameters mismatch, X_{∞_0}, Q_0, L_{∞_0} and R_0 vary up to 30% and M_0 varies up to 200 %, then a uniformly distributed stochastic noise between -0.2 mm and 0.2 mm is added to the position.

The controller performance and voltage control input are plotted in Fig. 5. Qualitatively, our simulation results show in Fig. 5b, 5d and 5f that the tracking error immediately converges with exponential form, into a small region of 0.3 mm, by a small root mean square error of 0.09 mm and rapid responses are achieved as shown in Fig 5a, 5c and 5e. It also illustrates in Fig. 5g that the control effort changes rapidly to ensure a fast response, when the disturbance, parameters

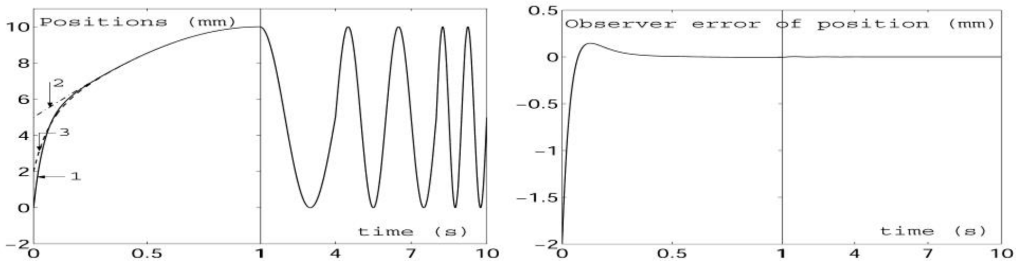

(a) (b)

(a) Positions dynamic. 1 – Actual position, 2 – reference, 3 – estimated position; (b) observer error

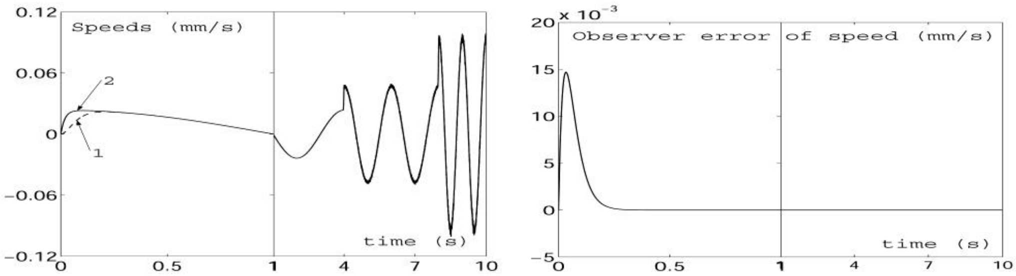

(c) (d)

(c) Speeds dynamic. 1 – Estimated speed, 2 – actual speed; (d) observer error

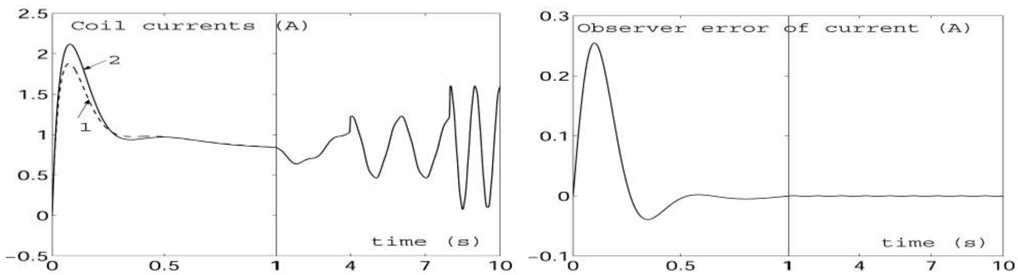

(e) (f)

(e) Coil currents dynamic. 1 – Estimated coil current, 2 – actual coil current; (f) observer error

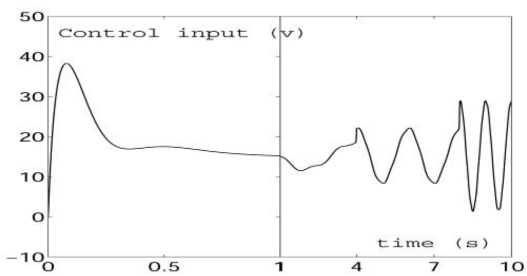

(g) Control input dynamic

Fig. 4. Controller performance, test one

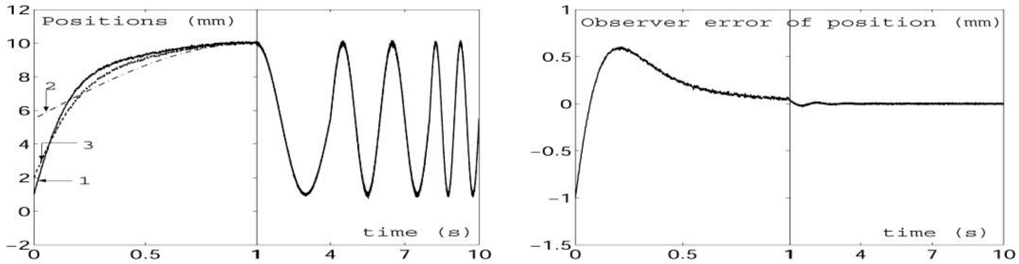

(a) (b)

(a) Positions dynamic. 1 – Actual position, 2 – reference, 3 – estimated position; (b) observer error

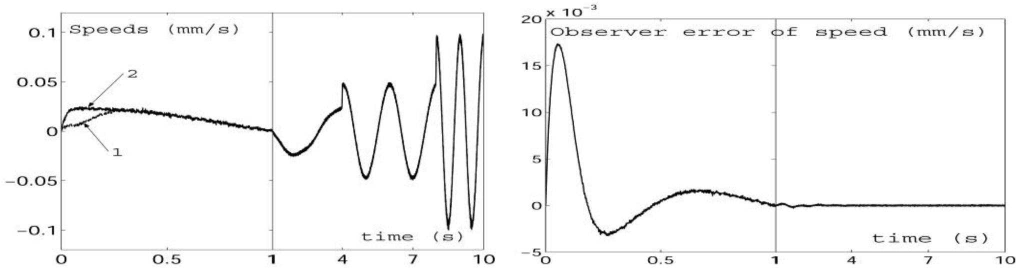

(c) (d)

(c) Speeds dynamic. 1 – Estimated speed, 2 – actual speed; (d) observer error

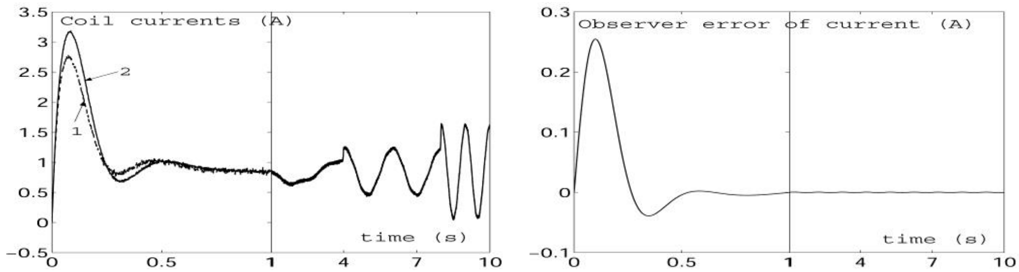

(e) (f)

(e) Coil currents dynamic. 1 – Estimated coil current, 2 – actual coil current; (f) observer error

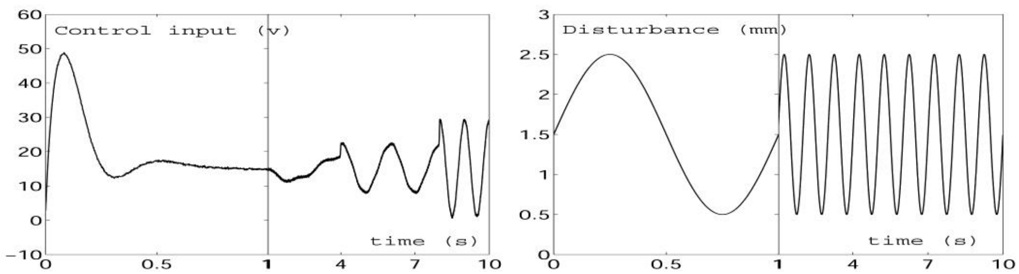

(g) Control input dynamic; (h) disturbance variation

Fig. 5. Controller performance, test two

mismatch and sensor noise are applied at the initial time. Then this controller ensures robust performance in this pre-defined framework, therefore, this result demonstrates the effectiveness of the controller.

8. Conclusion

In this paper, the robust nonlinear control for a magnetic levitation system using the CDM approach with backstepping technique and the nonlinear observer has been proposed. The Lyapunov analysis indicated that the errors in the completely closed loop system, controller, and observers converge to zero exponentially.

The proposed controller is applied in a discrete form with the Euler method. The sampling time is kept adequately small so that the discrete model resembles the continuous time model property.

The proposed control algorithm was found to generate better tracking performance and tolerable control effort. This superior performance is due to the fact that all the effect of parameters mismatch, disturbance and sensor noise are compensated with suitable feedback gains values.

The future research on this topic aims to propose the use of a reduced-order nonlinear observer with a CDM-backstepping controller.

References

[1] Vinodh K.E., Jerome J., *Algebraic Riccati equation based Q and R matrices selection algorithm for optimal LQR applied to tracking control of 3rd order magnetic levitation system*, Archive of Electrical Engineering, vol. 65, no. 1, pp. 151–168 (2016).

[2] Yang Z.J., Miyazaki K., Kanae S., *Wada K., Robust position control of a magnetic levitation system via dynamic surface control technique*, IEEE Transactions on Industrial Electronics, vol. 51, no. 1, pp. 26–34 (2004).

[3] Yang Z.J., Fukushima Y., Kanae S., Wada K., *Robust non-linear output-feedback control of a magnetic levitation system by K-filter approach*, IET Control Theory and Applications, vol. 3, no. 7, pp. 852–864 (2009).

[4] Teodorescu C.S., Sakamoto N., Olaru S., *Controller design for sine wave tracking on magnetic levitation system: a comparative simulation study*, IEEE International Conference on Control Applications, Yokohama, Japan, pp. 2231–2236 (2010).

[5] Hamamci S.E., *A robust polynomial based control for stable processes with time delay*, Electrical Engineering, vol. 87, pp. 163–172 (2005).

[6] Ali R., Mohamed T.H., Qudaih Y.S., Mitani Y., *A new load frequency control approach in an isolated small power systems using coefficient diagram method*, Electrical Power and Energy Systems, vol. 56, pp. 110–116 (2014).

[7] Mohamed T.H., Shabib G., Ali H., *Distributed load frequency control in an interconnected power system using ecological technique and coefficient diagram method*, Electrical Power and Energy Systems, vol. 82, pp. 496–507 (2016).

[8] Bhusnur S., *Effect of stability indices on robustness and system response in coefficient diagram method*, International Journal of Research in Engineering and Technology, vol. 4, no. 10, pp. 282–287 (2015).

[9] Bernard M.Z., Mohamed T.H., Qudaih Y.S., Mitani Y., *Decentralized load frequency control in an interconnected power system using coefficient diagram method*, Electrical Power and Energy Systems, vol. 63, pp. 165–172 (2014).

[10] Chang Y., Cheng C.C., *Block backstepping control of multi-input nonlinear systems with mismatched perturbations for asymptotic stability*, International Journal of Control, vol. 83, no. 10, pp. 2028–2039 (2010).

[11] Ma R., Zhao S., Wang M., *Global robust stabilisation of a class of uncertain switched nonlinear systems with dwell time specifications*, International Journal of Control, vol. 87, no. 3, pp. 589–599 (2014).

[12] Ghommam J., Saad M., *Backstepping based cooperative and adaptive tracking control design for a group of underactuated AUVs in horizontal plan*, International Journal of Control, vol. 87, no. 5, pp. 1076–1093 (2014).

[13] Hong Y., Zheng-jin F., Xu-yong W., *Nonlinear control for a class of hydraulic servo system*, Journal of Zhejiang University Science, vol. 5, no. 11, 1413–1417 (2004).

[14] Morawiec M., *Dynamic variables limitation for backstepping control of induction machine and voltage source converter*, Archive of Electrical Engineering, vol. 61, no. 3, pp. 389–410 (2012).

[15] Ker C.C., Lin C.E., Wang R.T., *Tracking and balance control of ball and plate system*, Journal of the Chinese Institute of Engineers, vol. 30, no. 3, pp. 459–470 (2007).

[16] Pettersen K.Y., Nijmeijer H., *Underactuated ship tracking control: Theory and experiments*, International Journal of Control, vol. 74, no. 14, pp. 1435–1446 (2001).

[17] Yu Y., Zhong Y.S., *Robust backstepping output tracking control for siso uncertain nonlinear systems with unknown virtual control coefficients*, International Journal of Control, vol. 83, no. 6, pp. 1182–1192 (2010).

[18] Won D., Kim W., *Disturbance observer based backstepping for position control of electrohydraulic systems*, International Journal of Control Automation and Systems, vol. 13, pp. 488–493 (2015).

[19] Pagilla P.R., Zhu Y., *Controller and observer design for lipschitz nonlinear systems*, Proceeding of the American Control Conference, Boston, United State of America, pp. 2379–2384 (2004).